Electronic and FTIR Spectroscopy of Controlled Chain Length Pristine and Iodine-Doped Permethylazine Oligomers

Bradford Charles Sherman, Brian K. Schmitz, and William B. Euler*

Department of Chemistry, University of Rhode Island, Kingston, Rhode Island 02881

Received January 18, 1995[⊗]

The electronic spectroscopy of a series of controlled chain length permethylazine oligomers, $H_2N[N{=}C(CH_3)C(CH_3){=}N]_xNH_2$ (x = 1-5, 7, 11), is examined in solution and as thin films. As the chain length is increased, evidence for the four π bands expected from the dimeric repeat unit is found, and this is corroborated by Hartree-Fock calculations at the 6-31G* level of the monomer (x = 1) and dimer (x = 2) in this series. In the thin film and in polar solvents a delocalization limit of about four repeat units is suggested, in agreement with FTIR results. Upon doping with gas-phase iodine, thin films of all of these oligomers (x > 2) develop the spectral signature of triiodide and this can be compensated for with ammonia gas. FTIR analysis of the iodine-doped thin films show that the only observed change is the development of a peak at 1505 cm^{-1} and that the basic geometry of the oligomers is unchanged. These results are interpreted as the formation of iodonium complexes bound to the imine nitrogen. This eliminates the bipolaron interpretation of similar spectral features found previously in iodine-doped polyazines since these oligomers are of insufficient chain length to support a bipolaron.

Introduction

Linear polymers with extended conjugation have been intensively studied in a variety of materials.[1-20] One fruitful avenue of study in these types of materials is the spectroscopy of well-defined controlled chain length oligomers which allows for observation of the development of the electronic and geometric structure as a function of the number of repeat units. Theoretical calculations reveal a chain length dependence of roughly $1/x$ on the bandgaps and ionization potentials of most conducting polymers.[21,22] Recent studies on polyacetylene have indicated the conjugation length in this material is on the order of 60 double bonds,[23,24] while for other polymers such as polythiophene[23] or polyaniline[24] the conjugation length appears to be much shorter.

Our interests have been in the polyazine, $[N{=}C(R){-}C(R){=}N]_x$, family of polymers.[25-32] These materials are formally isoelectronic to polyacetylene but, because of the presence of the nitrogen atoms, have considerably different properties, most notably good environmental stability in both the pristine and doped states. The electronic spectroscopy of polyazines is also expected to be quite different from that of polyacetylene for two reasons. First, the nitrogen atoms expand the number of orbitals in the repeat unit so that as many as four π-π^* band-to-band transitions can be expected.[32] Second, the lone pairs on the nitrogen atoms give the possibility of n-π^* transitions. An isolated imine

[⊗] Abstract published in *Advance ACS Abstracts,* March 15, 1995.

(1) Shirakawa, H.; Louis, E. J.; MacDiarmid, A. G.; Chiang, C. K.; Heeger, A. J. *J. Chem. Soc., Chem. Commun.* **1978**, 578.
(2) Fincher, C. R.; Ozaki, M.; Tanaka, M.; Peebles, D.; Lauchlan, L.; Heeger, A. J.; MacDiarmid, A. G. *Phys. Rev. B* **1979**, *20*, 1589.
(3) Chien, J. C. W. *Polyacetylene*; Academic Press: New York, 1984.
(4) Roth, S.; Bleier, H. *Adv. Phys.* **1987**, *36*, 385.
(5) Krobryansky, V. M.; Tereshko, E. A. *Synth. Met.* **1991**, *39*, 367.
(6) Shacklette, L. W.; Chance, R. R.; Ivory, D. M.; Miller, G. G.; Baughman, R. H. *J. Phys. Chem.* **1979**, *71*, 1506.
(7) Brédas, J. L.; Thémans, B.; Fripiat, J. G.; André, J. M. Chance, R. R. *Phys. Rev. B* **1984**, *29*, 6761.
(8) Pelous, Y.; Froyer, G.; Hérold, C.; Lefrant, S. *Synth. Met.* **1989**, *29*, E17.
(9) Kaneto, K.; Yoshino, K.; Inuishi, Y.; *Solid State Commun.* **1983**, *46*, 389.
(10) Chung, T.-C.; Kaufman, J. H.; Heeger, A. J.; Wudl, F. *Phys. Rev. B* **1984**, *30*, 702.
(11) Elsenbaumer, R. L.; Jen, K. Y.; Miller, G. G.; Shacklette, L. W. *Synth. Met.* **1987**, *18*, 277.
(12) Ruiz, J. P.; Gieselman, M. B.; Nayak, K.; Marynick, D. S.; Reynolds, J. R. *Synth. Met.* **1989**, *28*, C481.
(13) Street, G. B.; Clarke, T. C.; Krounbi, M.; Kanazawa, K.; Lee, V.; Pfluger, P.; Scott, J. C.; Weiser, G. *Mol. Cryst. Liq. Cryst.* **1982**, *83*, 253.
(14) Scott, J. C.; Pfluger, P.; Krounbi, M. T.; Street, G. B. *Phys. Rev. B* **1983**, *28*, 2140.
(15) Brédas, J. L.; Scott, J. C.; Yakushi, K.; Street, G. B. *Phys. Rev. B* **1984**, *30*, 1023.
(16) McManus, P. M.; Yang, S. C.; Cushman, R. J. *J. Chem. Soc., Chem. Commun.* **1985**, 1556.
(17) Euler, W. B. *Solid State Commun.* **1986**, *57*, 857.
(18) Epstein, A. J.; Ginder, J. M.; Zuo, F.; Bigelow, R. W.; Woo, H.-S.; Tanner, D. B.; Richter, A. F.; Huang, W.-S.; MacDiarmid, A. G. *Synth. Met.* **1987**, *18*, 303.
(19) Geniès, E. M.; Boyle, A.; Lapkowski, M.; Tsintavis, C. *Synth. Met.* **1990**, *36*, 139.
(20) Syed, A. A.; Dinesan, M. K. *Talanta* **1991**, *38*, 815.
(21) Brédas, J. L.; Silbey, R.; Boudreaux, D. S.; Chance, R. R. *J. Am. Chem. Soc.* **1983**, *105*, 6555.
(22) Lahti, P. M.; Obrzut, J.; Karasz, F. E. *Macromolecules* **1987**, *20*, 2023.
(23) Park, L. Y.; Ofer, D.; Gardner, T. J.; Schrock, R. R.; Wrighton, M. S. *Chem. Mater.* **1992**, *4*, 1388.
(24) Samuel, I. D. W.; Ledoux, I.; Dhenaut, C.; Zyss, J.; Fox, H. H.; Schrock, R. R.; Silbey, R. J. *Science* **1994**, *265*, 1070.
(25) Hauer, C. R.; King, G. S.; McCool, E. L.; Euler, W. B.; Ferrara, J. D.; Youngs, W. J. *J. Am. Chem. Soc.* **1987**, *109*, 5760.
(26) Euler, W. B. *J. Phys. Chem.* **1987**, *91*, 5795.
(27) Euler, W. B.; Roberts, J. E. *Macromolecules* **1989**, *22*, 4221.
(28) Euler, W. B. *Chem. Mater.* **1990**, *2*, 209.
(29) Chaloner-Gill, B.; Cheer, C. J.; Roberts, J. E.; Euler, W. B. *Macromolecules* **1990**, *23*, 4597.
(30) Chaloner-Gill, B.; Euler, W. B.; Roberts, J. E. *Macromolecules* **1991**, *24*, 3074.
(31) Chaloner-Gill, B.; Euler, W. B.; Mumbauer, P. D.; Roberts, J. E. *J. Am. Chem. Soc.* **1991**, *113*, 6831.
(32) Sherman, B. C.; Euler, W. B. *Chem. Mater.* **1994**, *6*, 899.

0897-4756/95/2807-0806$09.00/0

moiety typically has an n−π^* transition in the range 220−240 nm with a molar absorptivity (in solution) of about 100 L/mol cm[33−35] and a $\pi-\pi^*$ transition near 170 nm with a much larger absorptivity.[36] Conjugation of the imine to either a diimine (N=C−C=N) or to an azine (C=N−N=C) shifts the $\pi-\pi^*$ absorption considerably, to above 200 nm.[37] Our result here show similar trends but with the spectroscopic shifts stopping after about four repeat units.

Iodine doping of polyazines leads to moderately conducting materials.[25] On the basis of ^{15}N NMR results, we previously concluded that the charge carriers were due to bipolarons (formally, dinitrenium ions)[31] but this has been challenged based on high-level theoretical calculations.[38] We report here that iodine-doped oligomers and polymers have the same spectroscopic signatures in both the UV and IR regions; since the oligomers are too short to support bipolarons, it seems likely that the charge carriers in the polymers are not dinitrenium ions which could be expected to be stable only in the presence of extended delocalization. Instead, we propose that the iodine forms iodonium ions stabilized by complexation to the nitrogen atoms so that charge transport in the iodine-doped polymers is along the triiodide network and not along the polymer backbone.

Experimental Section

The permethyloligoazines ($H_2N[N=C(CH_3)C(CH_3)=N]_xNH_2$, x = 1−5, 7, 11) used in this study were prepared and characterized by previously published procedures.[25] Solution spectra were obtained in chloroform (Fisher optima used as received), methanol (Fisher Optima used as received), and hexane (Fisher Optima degassed with argon and dried over 4 Å molecular sieves). Shorter chain oligomers dissolved readily but the x = 7 and x = 11 species required 24−48 h of vigorous stirring to reach saturation. Spectra were recorded between 1100 nm and the respective solvent cutoffs (240 nm for chloroform, 205 nm for methanol, and 195 nm for hexane).

Thin films of each of the oligomers were prepared by spin-casting chloroform or methanol solutions of the oligomers onto optical quality quartz slides (NSG Precision Cells). Film thicknesses were estimated to be from 0.01 to 0.2 μm. For the thinner films (x = 7 or x = 11), up to 100 spectra were summed to achieve reasonable signal-to-noise ratios. Thin film spectra were recorded between 1100 and 190 nm.

Powdered samples diluted in KBr or NaCl were used for the FTIR analysis.

Doping and Compensation. Thin films cast on quartz substrates were placed in a sealed glass chamber physically separated from a layer of iodine crystals (Baker & Adamson resublimed reagent grade used as received). The films were allowed to react with the I_2 vapors at room temperature (21−27 °C) for various lengths of time; typically fully reacted films were obtained after 30−60 min. The films were then placed under vacuum to remove excess iodine.

For FTIR analysis the samples were pressed into NaCl pellets and reacted in the iodine chamber at room temperature for 30−60 min.

Compensation with NH_3(g) was accomplished by mounting a doped film in a glass chamber, purging with Ar for 15 min and then charging the chamber with anhydrous ammonia before sealing up to 48 h.

Table 1. Spectroscopic Results for $H_2N[N=C(CH_3)C(CH_3)=N]_xNH_2$ (λ_{max} in nanometers)

x	hexane	methanol	chloroform	thin film	I_2-doped thin film
1			293		
	261[a]	265	269[b]		
	222(sh)	222(sh)			
2				360	380
	300	301	299	315	300
	266	275	273	270	223
				210	
3	302	303	302	319	374
	269	273	272	277	300
4	310	302	307	314	369
	273	272	275	270	298
		226			
5	308	302	305	316	373
	271	270	271	272	301
	226				
7	311	306	305	310	367
	273	272	273	271	300
	225	222			
11	306	302	303	307	364
	272	270	270	266	299
	230	225		222	216
PMPAZ[c]	306		308	310	368
	272		275	269	298
	222			223	

[a] log ϵ = 4.16 where ϵ is the absorption coefficient in units of L/mol cm. [b] log ϵ = 3.97. [c] PMPAZ = $-[(N=C(CH_3)C(CH_3)=N)_{0.97}(N=C(CH_3)C(CH_2CH_2CH_3)=N)_{0.03}]_x-$; data taken from ref 32.

Instrumentation. The UV−vis spectra were recorded between 1100 and 190 nm on a Perkin-Elmer λ2 spectrophotometer operating in the double beam absorbance mode and employing the 2 nm curve smoothing function. IR spectra were obtained on a Perkin-Elmer Model 1650 FTIR spectrometer between 400 and 7800 cm^{-1} utilizing 2 cm^{-1} resolution and a N_2 purge.

Calculations. Hartree−Fock calculations were run using G90[39] with a 6-31G*[40] basis set at the HF/6-31G*//HF/6-31G* level on a VAX 4000 computer. Full geometry optimization was employed, but to reduce the size of the calculation, no methyl substituent groups were used.

Results and Discussion

The results for the UV−vis spectra for all of the samples studied are summaried in Table 1. Except for the monomer (x = 1; 2,3-butanedione dihydrazone, BDDH), all of the spectra are essentially solvent independent. This suggests that all of the observed resonances arise from $\pi-\pi^*$ transitions.

The BDDH spectra in hexane (shown in Figure 1) and methanol are similar: an intense maximum near 265 nm with a distinct shoulder at 222 nm. BDDH is a planar, C_{2h}, molecule[25] and is expected to have only a single low energy $\pi-\pi^*$ transition. Further, the lone pairs on amine nitrogens can conjugate into the π system causing a red shift of the absorption from a typical value found in a diimine. Thus, the major absorption at 265 nm is assigned as a $\pi-\pi^*$ transition and the shoulder is assigned as an n−π^* transition. In chloroform an additional peak is found at 293 nm. The origin of this transition is not known. It may arise from

(33) Bonnett, R. *J. Chem. Soc.* **1965**, 2313.
(34) Vocelle, D.; Dargelos, A.; Pottier, R.; Sandorfy, C. *J. Chem. Phys.* **1977**, *66*, 2860.
(35) Sandorfy, C. *J. Photochem.* **1981**, *17*, 297.
(36) Jaffé, H. H.; Orchin, M. *Theory and Applications of Ultraviolet Spectroscopy*; Wiley: New York, 1962.
(37) Barany, H. C.; Braude, E. A.; Pianka, M. *J. Chem. Soc.* **1949**, 1898.
(38) Dudis, D. S.; Yeates, A. T.; Kost, D.; Smith, D. A.; Medrano, J. *J. Am. Chem. Soc.* **1993**, *115*, 8770.
(39) Frisch, M. J.; Head-Gordon, M.; Tracks, G. W.; Foresman, J. B.; Schlegel, H. B.; Ragavachari, K.; Robb, M. A.; Binkley, J. S.; Gonzalez, C.; Defrees, D. J.; Fox, D. J.; Whiteside, R. A.; Seeger, R.; Melius, C. F.; Baker, J.; Martin, R. L.; Kahn, L. R.; Stewart, J. J. P.; Topial, S.; Pople, J. A. *Gaussian90*; Gaussian, Inc.: New York, 1990.
(40) Hariharan, P. C.; Pople, J. A. *Theor. Chim. Acta* **1973**, *28*, 213.

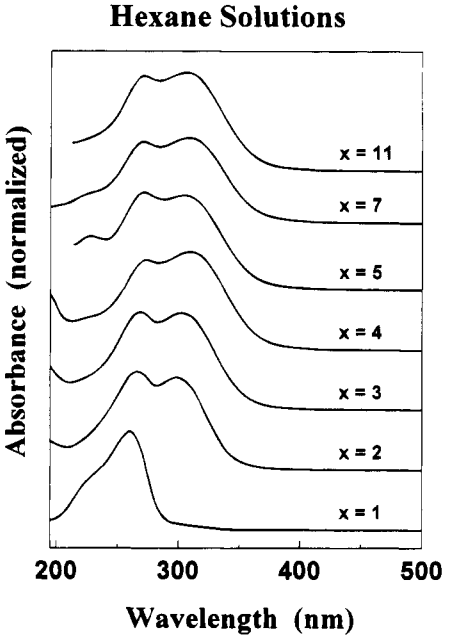

Figure 1. UV–vis spectra of hexane solutions of $H_2N[N{=}C(CH_3)C(CH_3){=}N]_xNH_2$ oligomers. The low energy absorption peak red shifts for $x = 1$ to $x = 4$ but little change is seen for $x > 4$.

the formation of π dimers or some other weakly associated species. However, it is not due to oligomerized impurities since a chloroform solution of BDDH could be evaporated and redissolved in methanol to give a typical methanol spectrum having no features at 293 nm.

As demonstrated in Figure 1, for all of the oligomers a similar spectrum in hexane is found: two major features near 300 and 275 nm, a weak peak or shoulder near 225 nm, and a shoulder near the high-energy spectral limit with an intensity that depends noticeably on the chain length. In addition to the solvent invariance, added glacial acetic acid had no effect on the spectral features for any of these samples (a similar experiment for BDDH caused rapid decomposition in solution so was not informative) suggesting that all of the major peaks are primarily π–π^* transitions with n–π^* transitions hidden underneath the absorption envelopes.

As the chain length is increased there is a slight variation in both the λ_{max} and the relative intensities of the two major peaks. Except for $x = 5$, the intensity of the low-energy peak increases relative to that of the high energy peak as the chain length increases. More importantly, the peak maxima also red shift from $x = 1$ to $x = 4$, and then no further shifts are found. This is shown in Figure 2 where the energies of the peak maxima are plotted as a function the inverse of the number of repeat units. The plot levels off at roughly $x = 4$ for both maxima (and is essentially the same as found in polymers,[32] as indicated in Table 1) indicating that the conjugation length in polyazines is about eight double bonds. This is significantly less than the 60 double bonds estimated for polyacetylene and is a reflection of the importance of the nitrogen atoms in influencing the electronic properties in this polymer.

To better support our spectral assignments, Hartree–Fock calculations were performed on $x = 1$ and $x = 2$ molecules with no methyl substituents. These results

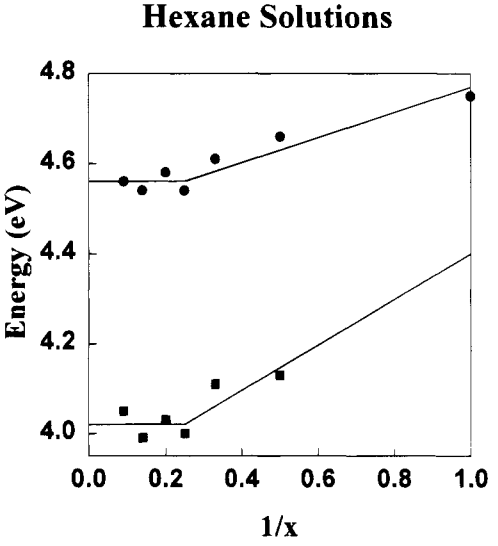

Figure 2. Plot of the peak maxima vs the inverse of the number of repeat units. The solid lines are drawn as guides for the eye and show the break at $x = 4$ for both absorptions.

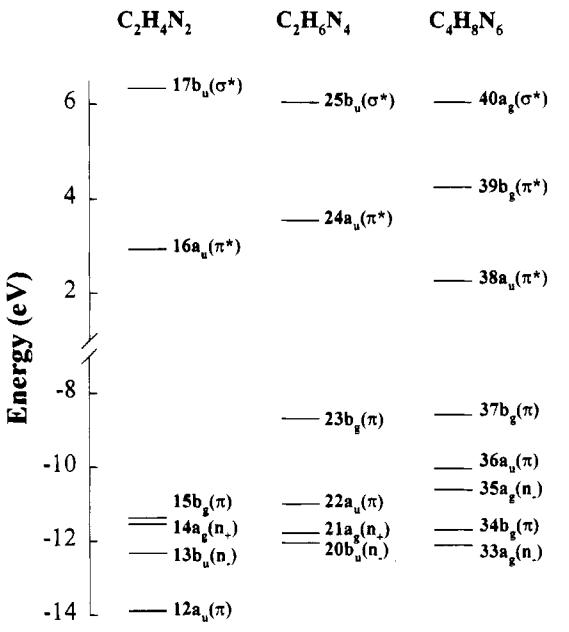

Figure 3. Energy level diagram in the valence region for $x = 1$ (HN=CHCH=NH, $C_2H_4N_2$ and $H_2NN{=}CHCH{=}NNH_2$, $C_2H_6N_4$) and $x = 2$ ($H_2NN{=}CHCH{=}NN{=}CHCH{=}NNH_2$) oligomers at the HF/6-31G*//HF/6-31G* level. Orbitals are labeled as lone pair (n) or π as well as their irreducible representation in C_{2h} symmetry.

are presented in Tables 2–4 and Figure 3. These calculations show that for BDDH ($C_2H_6N_4$ in Figure 3) the two lowest allowed transitions should be π–π^* ($23b_g^2 \rightarrow 23b_g^1 24a_u^1$, $^1A_g \rightarrow {}^1B_u$ in C_{2h}) and n–π^* ($21a_g^2 \rightarrow 21a_g^1 24a_u^1$, $^1A_g \rightarrow {}^1A_u$), as assigned. The dimer ($C_4H_8N_6$ in Figure 3) has a significantly reduced HOMO–LUMO gap, three allowed π–π^* ($37b_g^2 \rightarrow 37b_g^1 38a_u^1$, $34b_g^2 \rightarrow 34b_g^1 38a_u^1$, and $36a_u^2 \rightarrow 36a_u^1 39b_g^1$, all $^1A_g \rightarrow {}^1B_u$) transitions, and two n–π^* ($35a_g^2 \rightarrow 35a_g^1 38a_u^1$, and $33a_g^2 \rightarrow 33a_g^1 38a_u^1$, both $^1A_g \rightarrow {}^1A_u$) transitions, all in roughly the same energy regime. Although we find no convincing evidence for an n–π^* feature in the dimer spectrum, these could be expected to be buried under the π–π^* absorptions. Thus, the theoretical calculations are in full support of our spectroscopic assignments.

Table 2. Molecular Orbitals in the Valence Region for $H^3N^2{=}C^1H^4CH{=}NH$

orbital	energy (eV)	wave function[a]	comments
$11a_g$	−16.4079	$+0.3244C_1(2p_{x(1)}) - 0.1138C_1(2p_{x(2)}) + 0.1122C_1(2p_{y(1)})$ $-0.2228N_2(2p_{x(1)}) - 0.1208N_2(2p_{x(2)}) - 0.1831N_2(2p_{y(1)})$ $+0.1298N_2(2s_{(2)})$	C−N σ
$12a_u$	−13.8804	$+0.2786C_1(2p_{z(1)}) + 0.1746C_1(2p_{z(2)})$ $+0.2703N_2(2p_{z(1)}) + 0.1951N_2(2p_{z(2)})$	imine π
$13b_u$	−12.3144	$-0.1219C_1(2p_{x(1)}) - 0.1991C_1(2s_{(2)})$ $+0.3796N_2(2p_{y(1)}) + 0.2896N_2(2p_{y(2)})$ $-0.1124N_2(2s_{(1)}) - 0.1904N_2(2s_{(2)})$	lone pair n−
$14a_g$	−11.5291	$+0.1904C_1(2p_{y(1)})$ $-0.3181N_2(2p_{y(1)}) - 0.2592N_2(2p_{y(2)})$ $+0.2361N_2(2s_{(2)})$ $-0.1136H_3(1s_{(1)}) + 0.1351H_4(1s_{(1)}) + 0.1787H_4(1s_{(2)})$	lone pair n+
$15b_g$	−11.3561	$+0.2266C_1(2p_{z(1)}) + 0.1773C_1(2p_{z(2)})$ $+0.3373N_2(2p_{z(1)}) + 0.2730N_2(2p_{z(2)})$	imine π
$16a_u$	2.9441	$-0.2470C_1(2p_{z(1)}) - 0.3734C_1(2p_{z(2)})$ $+0.3122N_2(2p_{z(1)}) + 0.2730N_2(2p_{z(2)})$	imine π^*
$17b_u$	6.3394	$-0.3507C_1(2p_{x(2)}) - 0.1279C_1(2p_{y(1)}) - 0.2439C_1(2p_{y(2)})$ $-0.5525C_1(2s(2))$ $+0.2867N_2(2p_{x(2)}) - 0.3137N_2(2p_{y(2)})$ $-0.9579N_2(2s_{(2)})$ $+1.0562H_3(1s_{(2)}) + 0.7088H_4(1s_{(2)})$	σ^*
$18a_g$	6.8781	$+0.3410C_1(2p_{x(2)}) + 0.1350C_1(2p_{y(1)}) + 0.6690C_1(2p_{y(2)})$ $+0.3652C_1(2s_{(2)})$ $-0.1580N_2(2p_{x(1)}) - 0.2716N_2(2p_{x(2)}) + 0.2919N_2(2p_{y(2)})$ $+1.1362N_2(2s_{(2)})$ $-1.1121H_3(1s_{(2)}) - 0.8681H_4(1s_{(2)})$	σ^*

[a] The Gaussian basis for the C and N 2s and 2p and the H 1s orbitals are split into two parts labeled with subscripts (1) or (2). The z axis for these orbitals is perpendicular to the plane of the molecule. Only basis orbitals with coefficients greater than 0.1 are given. Atoms are labeled as the superscripts given in the title molecule and the other half of the molecular orbital function can be found by using the symmetry (as given for the C_{2h} point group).

Table 3. Molecular Orbitals in the Valence Region for $H^5H^4N^3N^2{=}C^1H^6CH{=}NNH_2$

orbital	energy (eV)	wave function[a]	comments
$19b_g$	−14.6836	$-0.1097C_1(2p_{z(1)})$ $-0.2328N_2(2p_{z(1)}) - 0.1504N_2(2p_{z(2)})$ $-0.2896N_3(2p_{z(1)}) - 0.2148N_3(2p_{z(2)}) + 0.1052N_3(2s_{(1)})$	imine + amine lone pair π
$20b_u$	−12.0426	$-0.1070C_1(2p_{x(1)}) - 0.1020C_1(2p_{y(1)}) - 0.1087C_1(2s_{(2)})$ $+0.3765N_2(2p_{y(1)}) + 0.2851N_2(2p_{y(2)})$ $-0.1036N_2(2s_{(1)}) - 0.2053N_2(2s_{(2)})$ $-0.1255N_3(2p_{y(1)})$	imine lone pair n−
$21a_g$	−11.7648	$-0.1611C_1(2p_{y(1)})$ $+0.3111N_2(2p_{y(1)}) + 0.2419N_2(2p_{y(2)}) - 0.2334N_2(2s_{(2)})$ $-0.1173H_6(1s_{(1)}) - 0.1584H_6(1s_{(2)})$	imine lone pair n+
$22a_u$	−10.9836	$-0.2151C_1(2p_{z(1)}) - 0.1559C_1(2p_{z(2)})$ $+0.1014N_2(2p_{y(1)})$ $+0.3092N_3(2p_{z(1)}) + 0.2774N_3(2p_{z(2)})$	imine + amine lone pair π
$23b_g$	−8.6873	$+0.2216C_1(2p_{z(1)}) + 0.1851C_1(2p_{z(2)})$ $+0.2523N_2(2p_{z(1)}) + 0.2232N_2(2p_{z(2)})$ $-0.2759N_3(2p_{z(1)}) - 0.2698N_3(2p_{z(2)}) + 0.1088N_3(2s_{(2)})$	imine + amine lone pair π
$24a_u$	3.5466	$-0.2182C_1(2p_{z(1)}) - 0.3476C_1(2p_{z(2)})$ $+0.3394N_2(2p_{z(1)}) + 0.4559N_2(2p_{z(2)})$ $-0.1266N_3(2p_{z(2)}) + 0.2062N_3(2s_{(2)})$ $-0.1834H_4(1s_{(2)})$	imine π^*
$25b_u$	6.0414	$+0.1083C_1(2p_{z(1)}) + 0.2625C_1(2p_{z(2)}) - 0.1033C_1(2p_{x(2)})$ $-0.2181C_1(2p_{y(2)}) - 0.3479C_1(2s_{(2)})$ $-0.1347N_2(2p_{z(2)}) - 0.1023N_2(2p_{x(2)})$ $-0.2507N_3(2p_{z(2)}) + 0.1601N_3(2p_{x(2)}) - 0.1850N_3(2p_{y(2)})$ $-1.1151N_3(2s_{(2)})$ $+0.9011H_4(1s_{(2)}) + 0.6198H_5(1s_{(2)}) + 0.4104H_6(1s_{(2)})$	σ^*
$26a_g$	6.4822	$+0.1788C_1(2p_{x(2)}) + 0.3819C_1(2p_{y(2)}) - 0.1173C_1(2s_{(2)})$ $-0.1179N_2(2p_{z(2)}) + 0.2439N_2(2p_{x(2)}) + 0.2608N_2(2s_{(2)})$ $+0.1167N_3(2p_{z(1)}) + 0.3697N_3(2p_{z(2)}) - 0.1879N_3(2p_{x(2)})$ $+1.2999N_3(2s_{(2)})$ $-0.8785H_4(1s_{(2)}) - 0.8612H_5(1s_{(2)}) - 0.1930H_6(1s_{(2)})$	σ^*

[a] The Gaussian basis for the C and N 2s and 2p and the H 1s orbitals are split into two parts labeled with subscripts (1) or (2). The z axis for these orbitals is perpendicular to the plane of the molecule. Only basis orbitals with coefficients greater than 0.1 are given. Atoms are labeled as the superscripts given in the title molecule and the other half of the molecular orbital function can be found by using the symmetry (as given for the C_{2h} point group, which is the approximate symmetry).

Figure 3 also compares the effect of the amino end group. The molecular orbitals of a diimine with H terminators ($C_2H_4N_2$ in Figure 3) have significantly different energies. The lone pair of the amine terminators conjugate into the π system causing the two filled π orbitals and the lowest energy empty π^* orbital to rise in energy. This confirms that the unusually low-energy transition found in BDDH is a result of the end group. This effect should diminish as the chain length increases and the relative importance of the end group decreases.

Table 4. Molecular Orbitals in the Valence Region for $H^5H^4N^3N^2{=}C^1H^6C^2H^7{=}N^4N{=}CHCH{=}NNH_2$

orbital	energy (eV)	wave function[a]	comments
$33a_g$	−12.1003	$+0.1399C_1(2p_{y(1)}) + 0.1098C_2(2p_{x(1)})$	end imine
		$-0.3465N_2(2p_{y(1)}) - 0.2641N_2(2p_{y(2)})$	n−
		$-0.1025N_2(2s_{(1)}) - 0.2235N_2(2s_{(2)}) + 0.1121N_3(2p_{y(1)})$	
		$-0.1056H_6(1s_{(1)}) - 0.1228H_6(1s_{(2)})$	
$34b_g$	−11.6913	$+0.1408C_1(2p_{z(1)}) + 0.2132C_2(2p_{z(1)}) + 0.1514C_2(2p_{z(2)})$	imine +
		$+0.1112N_2(2p_{y(1)})$	amine
		$-0.2254N_3(2p_{z(1)}) - 0.1983N_3(2p_{z(2)})$	lone pair
		$+0.1763N_4(2p_{z(1)}) + 0.1329N_4(2p_{z(2)})$	π
$35a_g$	−10.5972	$-0.1035C_2(2p_{y(1)})$	central
		$+0.4139N_4(2p_{y(1)}) + 0.3281N_4(2p_{y(2)}) - 0.2208N_4(2s_{(2)})$	imine n−
		$-0.1412H_7(1s_{(2)})$	
$36a_u$	−10.0315	$-0.2321C_1(2p_{z(1)}) - 0.1824C_1(2p_{z(2)})$	imine +
		$-0.1712N_2(2p_{z(1)}) - 0.1451N_2(2p_{z(2)})$	amine
		$+0.2846N_3(2p_{z(1)}) + 0.2667N_3(2p_{z(2)})$	lone pair
		$+0.1076N_4(2p_{z(1)})$	π
$37b_g$	−8.5820	$-0.1694C_1(2p_{z(1)}) - 0.1455C_1(2p_{z(2)})$	imine +
		$+0.1814C_2(2p_{z(1)}) + 0.1533C_2(2p_{z(2)})$	amine
		$-0.1912N_2(2p_{z(1)}) - 0.1698N_2(2p_{z(2)})$	lone pair
		$+0.2070N_3(2p_{z(1)}) + 0.2047N_3(2p_{z(2)})$	π
		$+0.2234N_4(2p_{z(1)}) + 0.1927N_4(2p_{z(2)})$	
$38a_u$	2.2652	$+0.1113C_1(2p_{z(1)}) + 0.1797C_1(2p_{z(2)})$	π^*
		$+0.2440C_2(2p_{z(1)}) + 0.3161C_2(2p_{z(2)})$	
		$-0.2427N_2(2p_{z(1)}) - 0.3091N_2(2p_{z(2)})$	
		$+0.1118N_3(2p_{z(2)}) - 0.1066N_3(2s_{(2)})$	
		$-0.1883N_4(2p_{z(1)}) - 0.2439N_4(2p_{z(2)})$	
$39b_g$	4.2527	$-0.2012C_1(2p_{z(1)}) - 0.3421C_1(2p_{z(2)})$	π^*
		$-0.1394C_2(2p_{z(2)})$	
		$+0.2654N_2(2p_{z(1)}) + 0.3771N_2(2p_{z(2)})$	
		$+0.2338N_3(2s_{(2)})$	
		$+0.2366N_4(2p_{z(1)}) + 0.3138N_4(2p_{z(2)})$	
		$-0.2196H_4(1s_{(2)}) - 0.1004H_5(1s_{(2)})$	
$40a_g$	6.0540	$-0.1715C_1(2p_{z(2)}) - 0.1392C_1(2p_{x(2)}) - 0.2828C_1(2p_{y(2)})$	σ^*
		$+0.1478C_1(2s_{(2)}) + 0.1929C_2(2p_{z(2)}) + 0.1802C_2(2s_{(2)})$	
		$-0.1514N_2(2p_{x(2)}) + 0.1684N_2(2s_{(2)})$	
		$+0.2688N_3(2p_{z(2)}) + 0.1719N_3(2p_{x(2)}) - 0.1607N_3(2p_{y(2)})$	
		$+1.1659N_3(2s_{(2)})$	
		$-0.8984H_4(1s_{(2)}) - 0.6845H_5(1s_{(2)}) - 0.3121H_6(1s_{(2)})$	

[a] The Gaussian basis for the C and N 2s and 2p and the H 1s orbitals are split into two parts labeled with subscripts (1) or (2). The z axis for these orbitals is perpendicular to the plane of the molecule. Only basis orbitals with coefficients greater than 0.1 are given. Atoms are labeled as the superscripts given in the title molecule and the other half of the molecular orbital function can be found by using the symmetry (as given for the C_{2h} point group, which is the approximate symmetry).

As the chain length increases the π orbitals found in the dimer must start forming "bands" by $x = 4$ oligomers and further increases in chain length only change the density of states and not the energies. Further, the highest energy absorptions, below 230 nm, are likely associated with transitions between occupied bands to the second LUMO band, as suggested previously for propyl substituted polyazines.[32]

The situation changes quite dramatically when the oligomers are cast as thin films, as shown in Figure 4. Optical quality films of the monomer BDDH could not be achieved by spin-casting and the crystalline nature of the dimer led to irreducible spectra, depending on casting solvent and spinning speed; we presume this to be a nonpreferential and uncontrolled alignment of crystallites upon deposition onto the quartz slide. The major changes in the dimer spectra cast under differing conditions were in the relative intensities of the peaks while peak positions only changed slightly. The longer chain oligomers ($x > 2$) are largely amorphous so the results were completely reproducible. As can be seen from Figure 4 and Table 1, the spectra for $x = 4$, 5, 7, and 11 are all essentially the same as the polymer (the spectrum labeled PMPAZ in Figure 4, shown for comparison purposes, is a polyazine with about 98.5% methyl substituents and about 1.5% propyl substituents used to give the material solubility). Thus, as concluded from the solution spectra, the conjugation length in polyazines is about four repeat units, or about eight double bonds.

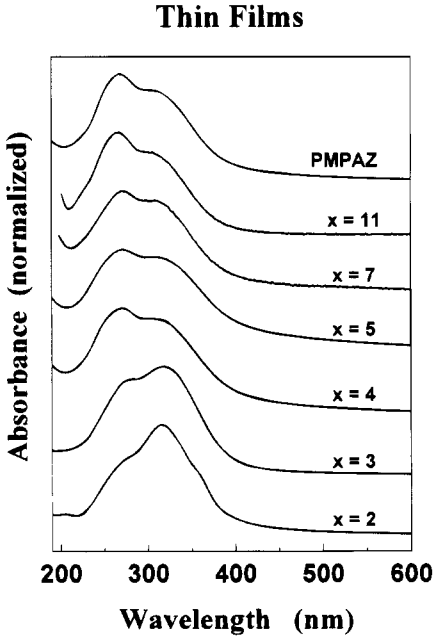

Figure 4. UV−vis spectra of thin films of $H_2N[N{=}C(CH_3)C(CH_3){=}N]_xNH_2$ oligomers. The spectrum labeled PMPAZ is for a polymer ($x > 20$) containing about 1.5% propyl substituents shown for comparison purposes.

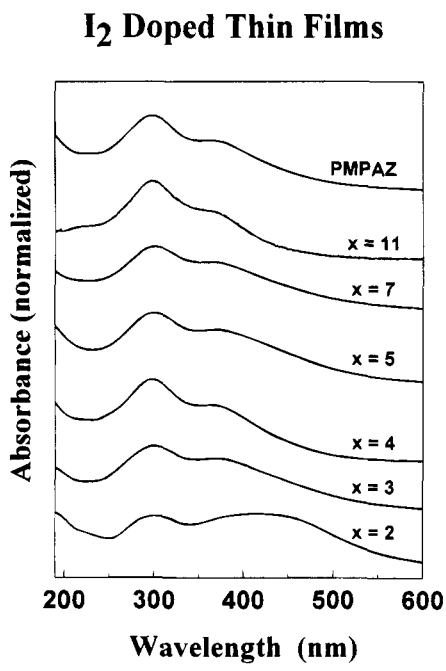

Figure 5. UV–vis spectra of thin films of $H_2N[N{=}C(CH_3)C(CH_3){=}N]_xNH_2$ oligomers doped with gas-phase iodine. The spectrum labeled PMPAZ is for an iodine-doped polymer ($x > 20$) containing about 1.5% propyl substituents shown for comparison purposes. All samples had been pumped extensively after reaction to remove free I_2.

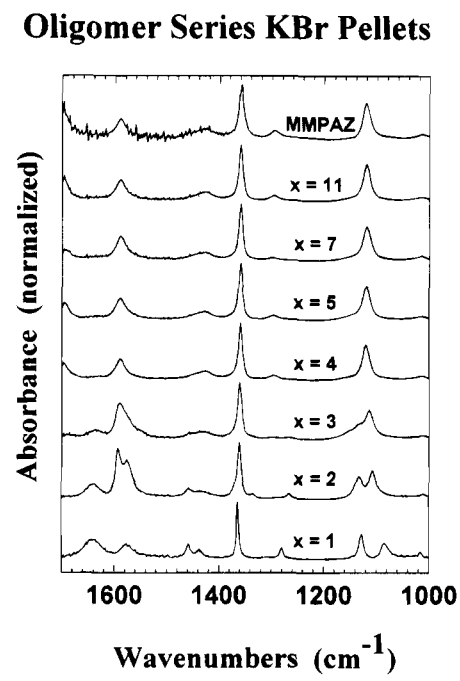

Figure 6. FTIR spectra of $H_2N[N{=}C(CH_3)C(CH_3){=}N]_xNH_2$ oligomers diluted in KBr pellets. The spectrum labeled MMPAZ is a polymer ($x > 45$) shown for comparison purposes.

The peak maxima of the thin film spectra do not show any region with a $1/x$ dependence, in contrast to the solution results. This indicates that the molecules are interacting with each other to some degree in the solid state. This conclusion is further justified by the observation that in the solution spectra the lower energy peak is generally found to be more intense than the higher energy peak; the reverse is true in the thin film spectra. This is consistent with the observation of π dimers in oligothiophenes.[41]

The thin films of these oligomers readily absorb and react with gas-phase iodine. After pumping to remove free, unreacted iodine the doped films are stable and give the spectra shown in Figure 5. All of these films have the major absorption near 300 nm and a second feature between 360 and 380 nm. These peaks are characteristic of the $^1\Sigma_u^+$ and $^1\Pi_u$ transitions of I_3^-, respectively.[42–44] The spectral features due to the conjugated imines are either gone or buried under the triiodide spectra. Thus, even in the shortest oligomers ($x = 2$) with as few as four double bonds, charge transfer has occurred. Since it is unlikely that a polaron or bipolaron would be stable for these short chain lengths, the cation must result from some process other than oxidation from the π orbitals or bands.

The I_2-doped thin films can be compensated with NH_3 gas. The reaction of the triiodide with ammonia completely removes the characteristic spectrum of the I_3^- and regenerates the spectrum characteristic of the conjugated imines, albeit at lower intensity. This process can be cycled several times with successive loss of the film, so either doping or dedoping is partially destroying the film. However, the observation that cycling can occur indicates that the imine structure is intact in the film that does remain on the surface.

To corroborate our structural conclusions, FTIR spectra of the oligomers were measured. Figure 6 shows the FTIR spectra between 1000 and 1700 cm^{-1} of these oligomers diluted in KBr pellets. The spectra for $x > 4$ are all essentially identical, again indicating that the conjugation length in these materials is about 8 double bonds. As the chain length is increased, the major changes in the IR spectrum are found in the 1550–1650 and the 1050–1150 cm^{-1} regions. The peaks found between 1550 and 1600 cm^{-1} are due to the C=N stretch, peaks found between 1600 and 1650 cm^{-1} are due to N–H rocking motions of the end groups (so become relatively less important as the chain length increases), and the peaks between 1050 and 1150 cm^{-1} are unassigned but are probably associated with single bond vibrations along the molecular backbone. The imine stretches are found at 1577 cm^{-1} for $x = 1$, 1576 and 1594 cm^{-1} for $x = 2$, 1590 cm^{-1} with a shoulder at about 1575 cm^{-1} for $x = 3$, and 1588 ± 1 cm^{-1} for all of the other materials. Thus, the end group imine stretches are found at 1576 cm^{-1} and the imine stretch in the bulk of the oligomer is found at 1588 cm^{-1}. The initial inclination in interpreting these values is to suggest that the conjugation between the imine and the end-group lone pair is more effective than the conjugation between imines along the chain. However, this is contradictory to the UV spectral results that clearly show shifts associated with conjugation even as the end groups disappear. A more likely interpretation is that the end-group imine stretches couple to the N–H rocking of the terminators (the IR allowed imine stretch in BDDH is of b_u symmetry as is one of the N–H rocking motions), shifting both resonances from the expected values near 1610 cm^{-1}. The unassigned peaks between 1050 and 1150 cm^{-1} also confirm the conjugation length: there

(41) Hill, M. G.; Penneau, J.-F.; Zinger, B.; Mann, K. R.; Miller, L. L. *Chem. Mater.* **1992**, *4*, 1106.
(42) Popov, A. I.; Swenson, R. F. *J. Am. Chem. Soc.* **1955**, *77*, 3724.
(43) Gabes, W.; Stufkens, D. J.; Gerding, H. *J. Mol. Struct.* **1973**, *17*, 329.
(44) Gabes, W.; Stufkens, D. J. *Spectrochim. Acta* **1974**, *30A*, 1835.

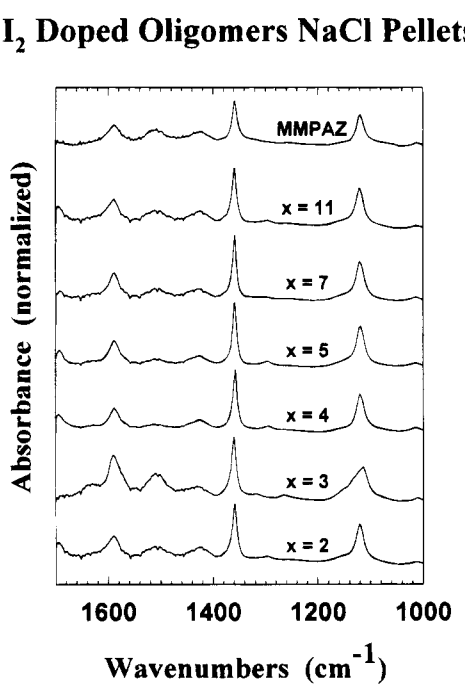

Figure 7. FTIR spectra of $H_2N[N{=}C(CH_3)C(CH_3){=}N]_xNH_2$ oligomers diluted in NaCl pellets and exposed to I_2 vapors. The spectrum labeled MMPAZ is a spectrum of an I_2-doped bulk polymer ($x > 45$) in a KBr pellet with a stoichiometry of 0.6 iodine atoms/repeat unit shown for comparison purposes.

are two peaks in the monomer (1085 and 1128 cm^{-1}), dimer (1108 and 1134 cm^{-1}), and trimer (1130 (sh) and 1113 cm^{-1}) with decreasing separations but for $x = 4$ and longer chains there is a single feature (1120 cm^{-1}).

These materials (except BDDH, where the monomer completely decomposed) were doped with iodine in NaCl pellets (NaCl was chosen for this experiment to minimize the possibility of I_2 reacting with the halide and altering the host lattice), and these spectra are shown in Figure 7. The spectra of the I_2 reacted materials are similar to the unreacted starting materials except for these two observations: the resolution is decreased sufficiently so that the doublets found in the undoped oligomers ($x = 2$ and $x = 3$) are now single peaks, and in all of the spectra a new peak is found at 1505 cm^{-1}. Originally in the polymer, this peak was assigned to a bipolaron absorption[25] but this is not likely in these short-chain oligomers.

To account for the observations, the reaction between these azine oligomers and iodine must be a disproportionation of I_2 into I^+ and I_3^- with the role of the azines being to stabilize the I^+ by complexation. The I^+ could bond to the azine through a nitrogen lone pair (similar to the pyridine-I_2 complex[45]) or the imine π bond:

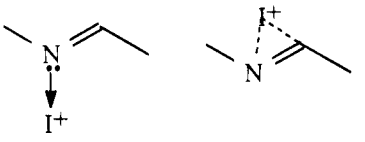

σ interaction π interaction

either structure could lead to a weakened imine bond (through a $p_\pi \rightarrow \pi^*$ backbond in the σ interaction or by directly attracting the electron density from the imine to the I^+ in the π interaction) accounting for the 1505 cm^{-1} IR peak. This implies that the conductivity found in the polymers is probably due to the iodine (as in iodine-doped poly(isoprenes)[46] and poly(propylene oxides)[47]) and not a mobile charge carrier on the polymer. Unfortunately, we were unable to test this hypothesis on I_2-doped oligomer thin films because in all cases the conductivity was below detection limits on our instrument.

Conclusions

UV–vis and FTIR spectroscopy on a series of controlled chain length oligomers of methyl-substituted polyazines has shown that the conjugation limit in these materials is about eight double bonds, significantly less than found in polyacetylene. The electronic spectroscopy originates entirely from π–π^* transitions in all of the materials with more than one repeat unit. The n–π^* transitions found in the monomer and suggested by the Hartree–Fock calculations were not observed.

Iodine doping of the oligomers led to the presence of triiodide in the UV–vis spectra and similar IR changes in all cases. To account for this, an azine assisted disproportionation of I_2 was proposed. The role of the azine was thought to be stabilization of the iodonium ion by complexation. This implies that the azine oligomers (and, consequently, the polyazines since all the spectral features are the same) do not form charge carriers and that any conductivity found in these materials is due to the iodine. Further experiments to confirm this hypothesis in the polymers are in progress.

Acknowledgment is made to the donors of the Petroleum Research Fund, administered by the American Chemical Society, for partial support of this work. We would also like to thank the Rhode Island Center for Thin Film and Interface Research for the loan of the spincaster used in this work.

CM9500317

(45) Jones, B.; Moody, G. J.; Thomas, J. D. R. *Inorg. Chem.* **1970**, *9*, 114.
(46) Chilkoti, A.; Ratner, B. D. *Chem. Mater.* **1993**, *5*, 786.
(47) Forsyth, M.; Shriver, D. F.; Ratner, M. A.; DeGroot, D. C.; Kannewurf, C. R. *Chem. Mater.* **1993**, *5*, 1073.